

## Scale Covariance of the Wrinkling Law of Turbulent Propagating Interfaces

A. Pocheau and D. Queiros-Condé

*Institut de Recherche sur les Phénomènes Hors Equilibre, S.252, Université Saint-Jérôme, 13397 Marseille, France*  
 (Received 17 February 1995; revised manuscript received 30 October 1995)

The physical process governing turbulent propagating interfaces is determined experimentally in scale space by analyzing the interface geometry and using the Kolmogorov cascade. Its scale covariance is evidenced for any scale range and any interface geometry, either Euclidean, fractal, or inbetween. This reveals a similarity of geometry formation more extended and more essential than the similarity of geometry itself.

PACS numbers: 61.43.Hv, 47.25.Gs, 47.70.Fw

The physics of interfaces within randomly stirred media involves many interesting topics: Interface evolution models a number of growth processes [1,2], interface geometry provides a diagnostic of turbulence [3,4], and interface dynamics reveals the enhancement of transport properties by turbulence [4,5]. To date, the statistics of turbulent interfaces has been characterized by exploiting the scale invariance of their geometry with respect to length or time [1–3,6]. This provides useful scaling relations in quasilaminar regimes [1,2] and in fully turbulent ones [3,6] but fails in evidencing universal laws in intermediate regimes. We conjecture that a possible origin of this breaking of universality traces back to the fact that these approaches address more a geometrical effect than a physical process.

The spirit of this Letter is to return to a causal analysis of geometry formation by focusing attention not on *geometry* itself but on the physical *process* actually generating it. Applied here to turbulent propagating interfaces, it allows us to evidence experimentally the invariance in scale space not of interface geometry, but of the *law* governing it. This scale covariance of geometry formation displays a wider universality than the usual scale invariance of geometry: It applies to any scale range and any regime, either Euclidean, fractal, or inbetween.

*Scale analysis.*—We consider an interface propagating in a turbulent fluid, the turbulence being assumed homogeneous and isotropic and the interface infinitely thin. In order to perform a scale analysis of the system, we introduce a geometrical series of length scales  $(L_i)_{i=0,I}$  with  $L_i/L_0 = a^i$  and  $a > 1$ ,  $L_0$  denoting the first wrinkling scale of interface and  $L_I$  the integral scale of turbulence.

Observing interfaces requires a field window  $W_j$  of size  $L_j$ , inside which a piece of interface is selected, and a resolution scale  $L_i < L_j$ , below which the geometrical details are ignored (Fig. 1). This turns out isolating the wrinkles belonging to the scale range  $[L_i, L_j]$  and thus addressing an effective interface labeled  $I_{i,j}$ . Its surface  $S_{i,j}$  is obtained by paving the actual interface with windows  $W_i$  of size  $L_i$  and by determining the number  $n_{i,j}$  of those belonging to  $W_j$ :  $S_{i,j} = n_{i,j}L_i^2$ . Owing to turbulence homogeneity and to the vanishing interface thickness, the velocity of the windows  $W_i$  are, in modulus

and in time average, the same:  $U_i$ . We define it as the normal velocity of the effective interface  $I_{i,j}$ .

Normal velocities may be linked to effective surfaces by expressing the volume swept per unit time by the interface, first with respect to  $U_i$  and then with respect to  $U_j$ :  $U_i S_{i,j} = U_j S_{j,j}$ . On the other hand, since  $S_{j,j} = L_j^2$  is the surface of the effective interface  $I_{i,j}$  projected on its mean normal direction, the ratio  $S_{i,j}/S_{j,j}$  corresponds to its wrinkling level, i.e., to its roughness  $R_{i,j}$ :  $R_{i,j} \equiv S_{i,j}/S_{j,j}$ . Altogether, these relations show that roughness describes the relative increase not only of spatial variables  $S_{i,j}$ , but also of dynamical ones  $U_i$ :

$$R_{i,j} \equiv \frac{S_{i,j}}{S_{j,j}} = \frac{U_j}{U_i}. \tag{1}$$

The classical scale analysis of interfaces turns out to fix the field scale  $L_j$  at the integral scale of turbulence  $L_I$  and study the variation of the roughness  $R_{i,I}$  with the scale ratio  $L_i/L_I$  in log-log coordinates. Here, roughness represents an effect of turbulence on interface geometry but scale ratios do not correspond to its cause since they are independent of its actual origin, the turbulence intensity.

The spirit of our approach consists of looking for a causal relation in this system. This requires first identifying in scale space a variable representative of the cause of wrinkling, the interface-turbulence interaction, and then linking it to its effect, the front roughness.

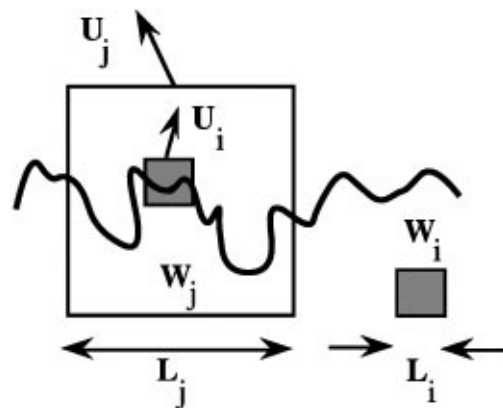


FIG. 1. Sketch of the scale analysis of interface.

We first define  $u'_{i,j}$  as the turbulence intensity (rms of velocity fluctuation) in the scale range  $[L_i, L_j]$  and make the following assumptions.  $A_1$ : the turbulent flow is scale invariant in the inertial range of turbulence.  $A_2$ : the squares of the turbulence intensities are additive with respect to scale ranges.  $A_3$ : the interface-turbulence interaction is local in scale space. Assumption  $A_1$  yields the power law  $u'_{i,i+1}/u'_{0,1} = (L_i/L_0)^K$ . Assumption  $A_3$  means that front wrinkles at a given scale are generated by vortices of the same scale only. It relies on the guess that, at a given scale, interface propagation is efficient enough to destroy the smaller scale tongues produced by turbulent mixing [7]. According to it, the roughness  $R_{i,j}$  of an effective interface  $I_{i,j}$  is a function of  $u'_{i,j}$  and  $U_i$  only, and thus of their ratio  $m_{i,j}$ :

$$R_{i,j} = \mathcal{R}_{i,j}(m_{i,j}), \quad (2)$$

$$m_{i,j} \equiv \frac{u'_{i,j}}{U_i}. \quad (3)$$

The so-called “mixing variables”  $m_{i,j}$  evaluate, in terms of velocities, the relative magnitude of turbulent mixing ( $u'_{i,j}$ ) with respect to propagation ( $U_i$ ). Thus they stand for the causes of front wrinkling. As the functions  $\mathcal{R}_{i,j}(\cdot)$  relate these causes to their effects, the roughness  $R_{i,j}$ , they represent the law governing the wrinkling process in scale space.

*Scale covariance.*—We have evidenced experimentally a fundamental property of the functions  $\mathcal{R}_{i,j}(\cdot)$  by the following procedure: Propagating interfaces are provided by premixed flames. They are studied in a closed chamber in which a grid turbulence is generated prior to ignition [8]. The net turbulence intensity  $u'$  in the inertial range of turbulence has been measured by laser velocimetry [8]. It is monitored by an ignition delay during which it decays according to a viscous time  $\tau_v = 136$  ms. The duration of propagation is short enough ( $\approx 10$  ms) for  $u'$  to be nearly frozen. Since both the Kolmogorov scale  $L_\eta$  and the wrinkling scales are larger than the flame thickness, fronts behave locally as planar laminar ones. In particular, their normal velocity  $U_N$  is a constant equal to that of planar flames. It is determined by physicochemical processes and is monitored here by the equivalence ratio  $\varphi$  and the dilution  $\delta$  of the mixture. The experiment involves the following parameter ranges: combustion volume  $10 \times 6 \times 6$  cm<sup>3</sup>, propane-air mixture ( $0.85 \leq \varphi \leq 1.30$ ,  $\delta = 0.15$  or  $0.21$ ), normal velocity at the observation time  $0.40 \leq U_N \leq 0.86$  ms<sup>-1</sup>,  $0.30 \leq u' \leq 0.93$  ms<sup>-1</sup>, and  $0.7 \leq u'/U_N \leq 2.2$ .

Flame fronts are visualized by tomography (Fig. 2) [9]. They display a geometry varying with the ratio  $m = u'/U_N$  from Euclidean ( $m < 1$ ) to fractal ( $m \approx 2$ , fractal dimension  $d_F \approx 2.4$ ). The functions  $\mathcal{R}_{i,j}(\cdot)$  may be determined from each of them since roughness  $R_{i,j}$  is measurable by image processing, normal velocities  $U_i$  derive from roughness by the relation (1) and turbulence intensities  $u'_{i,j}$  follow from the scaling law implied by  $A_1$ ,

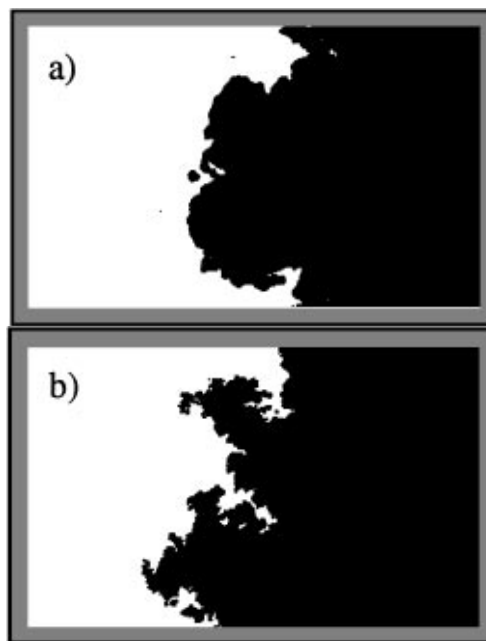


FIG. 2. Tomographic cuts of turbulent flame fronts  $6 \times 10$  cm wide: (a)  $u'/U_N = 0.71$ , (b)  $u'/U_N = 1.30$ .

$A_2$ , and the value of  $u'$ . However, using the multiplicative nature of roughness, we have avoided measuring all of them by deducing their value from a single series of measurements  $(R_{i,l})_{i=0,l}$ :  $R_{i,j} = R_{i,l}/R_{j,l}$ . Finally, in order to lower the experimental noise, we have averaged the roughness  $R_{i,l}$  along the interface and fitted them with respect to scale ratios  $L_i/L_l$  by a polynomial of order 3 in log-log coordinates.

For evidencing the wrinkling law, we first fix the resolution scale at the lowest wrinkling scale  $L_0$  and increase the observation scale  $L_j$ . This turns out accumulating progressively the effects of turbulent vortices of increasing size. The computation of the mixing variables  $m_{0,j} = u'_{0,j}/U_0$  from  $u'$  and  $U_N$  is performed as follows: Since the front is not yet wrinkled at the scale  $L_0$ ,  $U_0 = U_N$ ;  $u'_{0,j}$  may be expressed with respect to  $u'_{0,1}$  within the assumptions  $A_1$  and  $A_2$ ;  $u'_{0,1}$  may be identified with  $u'$  to a good accuracy because there is at least as scales inbetween  $L_l$  and  $L_0$  than inbetween  $L_0$  and the Kolmogorov scale  $L_\eta$  ( $L_l/L_0 > L_0/L_\eta \Rightarrow u'_{0,l} \approx u'_{\eta,l} = u'$ ). Plotting roughness versus mixing variables in square coordinates then yields a surprising result: At each equivalent ratio and dilution [e.g.,  $\varphi = 1.30$ ,  $\delta = 0.21$  in Fig. 3(a)] *all* the flames, either weakly wrinkled ( $m < 1$ ) or fractal-like ( $m > 1$ ,  $2.20 \leq d_F \leq 2.31$  for  $\varphi = 1.30$ ), generate for  $K = \frac{1}{2}$  the *same* curve as  $j$  varies. Since, at a given scale  $L_j$ , the values of  $m_{0,j}$  vary from flame to flame according to the value of  $m$ , this identity means that the functions  $\mathcal{R}_{0,j}(\cdot)$  are all the same, a linear law  $\mathcal{R}_0(\cdot)$  in the representation  $(m_{0,j}^2, R_{0,j}^2)$ :  $\mathcal{R}_{0,j}(\cdot) = \mathcal{R}_0(\cdot)$  with  $\mathcal{R}_0(x) = 1 + \beta x$ .

The existence of a single law  $\mathcal{R}_0(\cdot)$  for the whole family of scale range  $[L_0, L_j]$ ,  $0 < j \leq l$ , evidences an unexpected universal behavior of the wrinkling process.

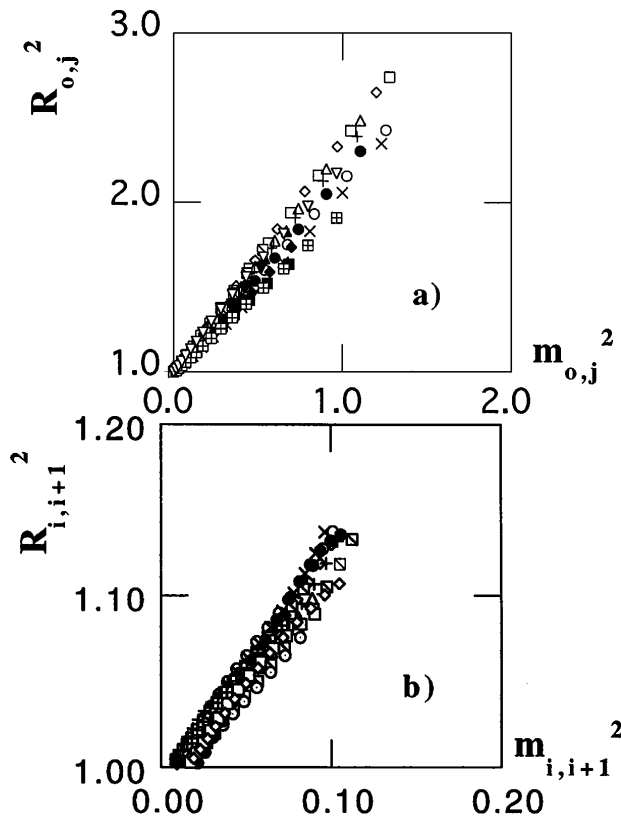


FIG. 3. Experimental determination of the wrinkling law in scale space:  $a = 1.2$ ,  $K = 1/2$ ,  $\varphi = 1.30$ ,  $\delta = 0.21$ ,  $0.6 \leq u'/U_N \leq 1.3$ , 14 flames, a symbol per flame. (a) Scale ranges  $[L_0, L_j]$ ,  $L_0$  fixed,  $L_j$  variable; (b) consecutive scale ranges  $[L_i, L_{i+1}]$ .

Its linear form in quadratic coordinates was already predicted in a previous work within assumptions  $A_2$  and  $A_3$  and the scale invariance of the wrinkling process [10]. It corresponds to a special property of the wrinkling law which, using (1), (3), and  $A_2$ , is evidenced here by the following equivalences:

$$R_{0,j}^2 = 1 + \beta m_{0,j}^2, \quad \forall j, \quad (4)$$

$$U_j^2 = U_0^2 + \beta u_{0,j}^2, \quad \forall j, \quad (5)$$

$$U_j^2 = U_i^2 + \beta u_{i,j}^2, \quad \forall i, \forall j, \quad (6)$$

$$R_{i,j}^2 = 1 + \beta m_{i,j}^2, \quad \forall i, \forall j. \quad (7)$$

Relation (7) shows that the expressions  $\mathcal{R}_{i,j}(\cdot)$  of the wrinkling law are independent of  $i$  and  $j$ :  $\mathcal{R}_{i,j}(\cdot) = \mathcal{R}(\cdot)$ . This means that changing scales preserves the form of the wrinkling law so that it is scale *covariant*. This includes a covariance by *global* changes ( $L_k \rightarrow a^p L_k = L_{k+p}$ ,  $\forall k$  with  $p$  constant) but also by *local* ones [ $L_k \rightarrow a^p L_k = L_{k+p}$ ,  $\forall k$  with  $p \equiv p(k)$ ]. They, respectively, express the impossibility of identifying either scales ( $L_k$ ) or scales ratios ( $L_{k'}/L_k$ ) from the wrinkling law, as required in a scale invariant system [10].

In order to test this property experimentally, we look for determining the wrinkling law in smaller scale ranges, the smallest ones available in scale space:  $[L_i, L_{i+1}]$ . The mixing variables  $m_{i,i+1} \equiv u'_{i,i+1}/U_i$  are easily computed from assumption  $A_1$ , which gives  $u'_{i,i+1}$ , and relation (1), which yields  $U_i = U_0 R_{0,i}$  where  $U_0 = U_N$ . Still in a quadratic representation ( $m_{i,i+1}^2, R_{i,i+1}^2$ ) and for  $K = 1/2$  we obtain, to the experimental accuracy [11], for *any* flame and *any* turbulence level, the *same* line as that previously derived for larger scale ranges [Fig. 3(b)]. This result directly evidences the scale covariance of the wrinkling process and shows its universality in scale space [12]. It finally confirms the relevance of the family of scale covariant laws (7).

Despite the fact that the covariant law is a line in both representations [Figs. 3(a) and 3(b)], Fig. 3(b) must not be confused with an enlargement of Fig. 3(a), the changes of coordinates from one representation to the other being actually nonlinear and nonlocal in scale space:  $R_{i,i+1}^2 = R_{0,i+1}^2/R_{0,i}^2$ ;  $m_{i,i+1}^2 = (m_{0,i+1}^2 - m_{0,i}^2)/R_{0,i}^2$ .

Owing to the limited available range of turbulence intensity ( $m \leq 2.2$ ,  $d_F \leq 2.4$ ) and to the experimental uncertainties, it is instructive to investigate the accuracy to which scale covariance is evidenced. For this, consider two noncovariant laws proposed in the literature, one at low turbulence level (8) [13] and the other at larger ones (9) [14]:

$$R_{0,j} = 1 + \frac{\beta}{2} m_{0,j}^2, \quad (8)$$

$$R_{0,j}^2 = \exp(\beta m_{0,j}^2/R_{0,j}^2). \quad (9)$$

The law (8) follows from the statement that the wrinkling amplitude in the scale range  $[L_0, L_j]$  is proportional to  $u'_{0,j}/U_N = m_{0,j}$  and from the subsequent derivation of the corresponding roughness at the dominant order in  $m_{0,j}$ . The law (9) is derived by renormalization of (8). Both are nondimensional and tangent to the covariant law (4) at low  $m_{0,j}$ . However, they differ from (4) regarding nonlinearity.

The plots of laws (8) and (9), together with that of the covariant one (4), are shown in Figs. 4(a) and 4(b) in the same representations and for the same ranges of data as in Figs. 3(a) and 3(b). As may be noticed by comparing Figs. 3(a) and 4(a), our experimental data could not actually decide between the noncovariant laws and the covariant one in the scale ranges  $[L_0, L_j]$ . However, changing scales so as to work with consecutive ones  $[L_i, L_{i+1}]$  produces dramatic variations of the noncovariant laws in Fig. 4(b) which largely exceed the experimental uncertainties of Fig. 3(b). This attests to the significance of the scale covariance observed experimentally.

The scale covariance of the wrinkling law follows from  $A_2$ ,  $A_3$ , and the scale invariance of the wrinkling process [10]. It is, however, independent of the scale invariance of the flow ( $A_1$ ) which is used here only as a useful means for approximating the turbulence intensities. The

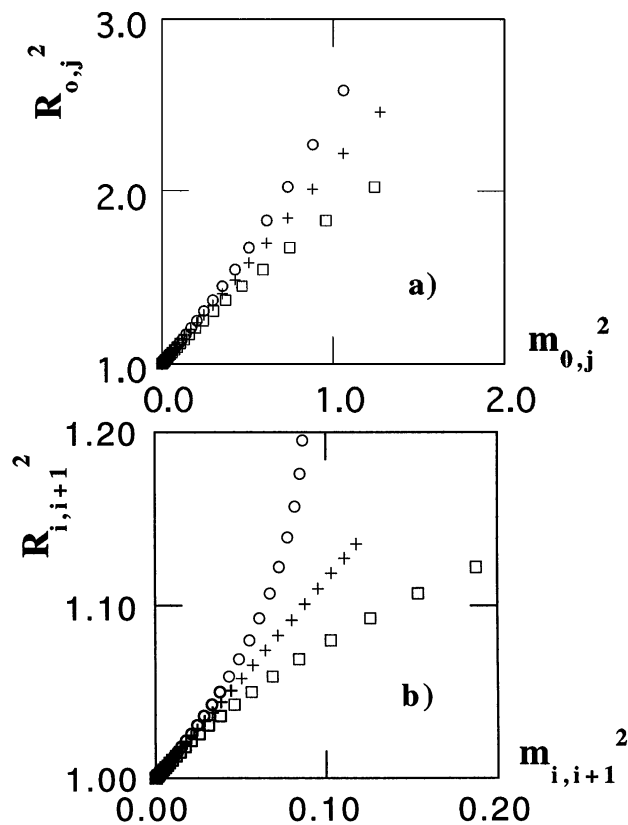


FIG. 4. Theoretical wrinkling laws (4) (crosses), (8) (circles), and (9) (squares) within the experimental scale range  $[L_0, L_I]$  for  $a = 1.2$  and  $u'/U_N \leq 1.3$ . (a),(b): same as in Fig. 3. In (b), the laws (8) and (9) even extend beyond the plotted range.

fact that a single exponent  $K = \frac{1}{2}$  yields covariance for all flames indicates that the corresponding power law is representative of the turbulent flow. The shift with respect to the usual value  $K = \frac{1}{3}$  of the Kolmogorov cascade shows an effect of combustion on turbulence. In particular, the temperature increase at the interface implies that the actual dissipation scale of the wrinkling vortices is the Kolmogorov scale in the (hot) burnt gases  $L_{\eta^*}$  instead of its much smaller value  $L_{\eta}$  in the (cold) fresh gases. This statement, confirmed by the fact that  $L_{\eta^*}$  is close to the first wrinkling scale  $L_0$ , implies that the range of wrinkling vortices is more dissipative than inertial. Its turbulence intensities then show a correction to the inertial range power law [15] which, in the present scales range, is well fitted by a power law, but with an exponent  $K = 0.53$  closer to  $\frac{1}{2}$  than to  $\frac{1}{3}$ .

The complete universality displayed by scale covariant laws bears some analogy with the extended self-similarity (ESS) recently evidenced in fully developed turbulence [16]. The ESS states that, given a statistical variable  $u$ , the scaling relation between its time-averaged moments  $\langle u^n \rangle \approx \langle u \rangle^{\xi(n)}$  is valid on a much larger scale range than the scaling relation between moments and scale  $\langle u^n \rangle(l) \approx l^{\xi(n)}$ . In the present case, a scaling relation between roughness  $R_{i,l}$  and scale  $L_i$  means a straight variation in log-log coordinates corresponding to a fractal regime. It

is thus restricted to the most turbulent flames and to their largest wrinkling scales. In contrast, the relation between roughness  $R_{i,j}$  and mixing variables  $m_{i,j}$  is valid on the whole range of wrinkling scales and for any turbulence level. It thus extends the domain of validity of universal laws as the ESS does in turbulence.

A causal approach of geometry formation has been applied to turbulent propagating interfaces. It has led the experimental evidence of the scale covariance of the law governing interface geometry. This property extends the usual concept of scale invariance of geometry to the laws governing form generation and so unifies the physical description of all interfaces, either Euclidean, fractal, or inbetween. Since scale covariance follows from scale invariance, its validity may be expected to be as widespread as scale similarity in out-of-equilibrium systems.

This work was supported by the E.E.C. (Joule Programme), the CNRS-PIRSEM, and the ADEME.

- [1] *Dynamics of Fractal Surfaces*, edited by F. Family and T. Vicsek (World Scientific, Singapore, 1991).
- [2] M. Kardar, G. Parisi, and Y-C. Zhang, *Phys. Rev. Lett.* **56**, 889–892 (1986).
- [3] K.R. Sreenivasan, *Annu. Rev. Fluid Mech.* **23**, 539 (1991).
- [4] E. Villermaux and Y. Gagne, *Phys. Rev. Lett.* **73**, 252–255 (1994).
- [5] P.D. Ronney, B.D. Haslam, and N.O. Rhys, *Phys. Rev. Lett.* **74**, 3804 (1995).
- [6] N. Peters, in *Proceedings of the 21st Combustion Symposium, Munich, West Germany, 1986* (The Combustion Institute, Pittsburgh, 1986), p. 1231; A. Kerstein, *Combust. Sci. Technol.* **60**, 441 (1988).
- [7] P. Clavin, in *Theory of Flames in Disorder and Mixing*, edited by E. Guyon *et al.* NATO Advanced Study Institutes, No. 152 (Kluwer Academic, Dordrecht, 1987), p. 293.
- [8] A. Floch, M. Trinité, F. Fisson, T. Kageyama, C. Kwon, and A. Pocheau, *Prog. Astronaut. Aeronaut.* **131**, 378 (1989).
- [9] L. Boyer, *Combust. Flame* **39**, 321 (1980).
- [10] A. Pocheau, *Phys. Rev. E* **49**, 1109 (1994).
- [11] As confirmed on test files generated by covariant laws, the shift with respect to the point (1,0) is an artifact of the data processing. It results from an artificial bending induced by the noncovariant nature of the polynomial fit of roughness versus scale in log-log coordinates. However, the relative difference of slopes from Figs. 3(a) to 3(b) does not exceed 5% for each flame.
- [12] As implied by (7), covariance is also evidenced for any other kinds of scale ranges, e.g.,  $[L_i, L_{i+2}]$ .
- [13] P. Clavin and F.A. Williams, *J. Fluid Mech.* **90**, 589–604 (1979).
- [14] V. Yakhot, *Combust. Sci. Technol.* **60**, 191–214 (1988).
- [15]  $u'_{\eta^*,i} \propto [1 - \exp\{-(L_i/L_{\eta^*})^{2/3}\}](L_i/L_{\eta^*})^{1/3}$ , as discussed in Ref. [4].
- [16] R. Benzi, S. Ciliberto, C. Baudet, R. Tripiccone, F. Massaioli, and S. Succi, *Phys. Rev. E* **48**, R29 (1993).